Article:
Gao, Y, Chai, W, Wang, L et al. (2016) Effect of friction and clearance on kinematics and contact mechanics of dual mobility hip implant. Proceedings of the Institution of Mechanical Engineers. Part H, Journal of Engineering in Medicine, 230 (1). pp. 39-49. ISSN: 0954-4119

https://doi.org/10.1177/0954411915617198

Effect of Friction and Clearance on Kinematics and Contact Mechanics of Dual Mobility Hip Implant

Yongchang Gao[1,4], Wei Chai[2,4], Ling Wang[1*], Manyi Wang[1], and Zhongmin Jin[1,3]

[1]State Key Laboratory for Manufacturing System Engineering, School of Mechanical Engineering, Xi'an Jiaotong University, 710054, Xi'an, Shaanxi, China;

[2]The Department of Orthopaedics, General Hospital of Chinese People's Liberation Army, 100853, Beijing, China;

[3]Institute of Medical and Biological Engineering, School of Mechanical Engineering, Uinversity of Leeds, LS2 9JT, UK;

[4]Both authors contributed equally to this work

* Corresponding author:

Associate Professor, Ling Wang

State Key Laboratory for Manufacturing System Engineering, School of Mechanical Engineering, Xi'an Jiaotong University

Tel.: +0-86-029-83395187

E-mail: menlwang@mail.xjtu.edu.cn

Abstract: The dual mobility hip implant has been introduced recently and increasingly used in total hip replacement to maintain the stability and reduce the risk of post-surgery dislocation. However, the kinematics and contact mechanisms of dual mobility hip implants have not been investigated in details in the literature. Therefore finite element method was adopted in the present study to investigate dynamics and contact mechanics of a typical metal-on-polymer dual mobility hip implant under different friction coefficient ratios between the inner and the outer articulations and clearances/interferences between the ultra-high-molecular-weight polyethylene liner and the metal back shell. A critical ratio of friction coefficients between the two pairs of contact interfaces was found to mainly determine the rotating surfaces. Furthermore, an initial clearance between the liner and the back shell facilitated the rotation of the liner while an initial interference prevented such a motion at the outer articulating interface. In addition, the contact area and the sliding distance at the outer articulating surface were markedly greater than those at the inner cup/head interface, potentially leading to extensive wear at the outer surface of the liner.

Key works: dual mobility hip implant; contact mechanics; dynamics ; friction coefficient; clearance/interference

1. introduction

Since metal-on-polymer artificial hip joints were introduced by Charnley in the 1960s, the total hip replacement has been advanced significantly and used successfully in orthopedics to cure severe hip diseases[1, 2]. However, aseptic loosening caused by long-term wear and dislocation are still two main problems which limit the clinical lifetime of artificial hip joints[3, 4]. Among various techniques to prevent dislocation, the dual mobility hip implants first introduced by Gilles showed excellent clinical outcome to

prevent dislocation and at the same time to allow a physiological range of motions[5-8]. Consequently, there is a growing interest in orthopedic communities to develop dual mobility hip implants.

The main difference between a dual mobility hip implant and a conventional one is that the liner of the dual mobility hip is not fixed onto its metal back shell, thus the liner has the potential to rotate with the head under some conditions. The outside of the liner and the metal shell should not have excessive sliding under normal walking conditions. Coupled with a large contact area at the interface between the liner and the metal backing, the rotation of the liner may lead to an excessive wear volume. Geringer[9] examined the wear volume of 12 retrieval dual mobility cups, and showed that wear occurred at both the inner and outer surfaces of the liner, and the average outer wear volume occupied over 40% of the average total wear volume(53.9 mm^3). These results were also consistent with those obtained by Adam et al.[10]. In 2010 Saikko tested the wear of both Stafit and Allofit Alpha dual mobility hip implants using a HUT-4 anatomic hip joint simulator, and found the average inner wear was about 20 $mg/10^6$ cycles, consistent with clinical observations[11]. In 2012, Loving tested the dual mobility hips using the MTS hip simulator under the conditions of normal range of motion and impingement(adjusted the initial position of the head neck and the liner to make them contact during the movement). The results showed that both the inner wear volume and volumetric wear rate were little different, and the average volume wear rate was only about 1.0 $mm^3/10^6$ cycles[12]. However, none of them reported the wear of the liner outer surface.

In contrast, Rowe reported a predominant outer motion[13]. In their following investigation, both inner

and outer motions were observed under different conditions[14]. Although the previous studies have showed different motion statuses and wear performances of dual mobility hip implants both in vivo and in vitro, to the best of authors' knowledge, there are no comprehensive analyses made on the dynamics and contact mechanics of a dual mobility hip implant. Consequently, the magnitudes of relative sliding distance and contact pressure as well as contact area of both two pairs of contact surfaces are still unknown for dual mobility hip implants, whereas these key data will directly determine the amount of volumetric and linear wear. There are a number of parameters that could influence this process, including the design parameters of the radii of the inner and outer bearing diameters and the clearances between the head and the liner and between the liner and the shell, the friction coefficients between the two interfaces, and the gait motions. In this first study, only the friction coefficients and clearances were focused. The aim of this study was to investigate the influences of friction coefficients and initial clearance/interference between the liner and the back shell on dynamics and contact mechanics of a typical dual mobility hip implant during a normal walking gait cycle.

2. Materials and methods

A conceptual dual mobility hip implant was modeled, including four main parts; cobalt-chromium-molybdenum (CoCrMo) alloy shell, ultra-high-molecular-weight polyethylene (UHMWPE) liner, head (CoCrMo) and stem(Ti alloy)(Fig.1(a) and (b)). The geometry and dimensions were adopted from previous studies[15-17]. The main dimensions and materials parameters are listed in Table

1. UHMWPE was modeled as non-linear elastic-plastic material according to Fregley and Kluess[18, 19],and its yield strength was 23.56 MPa. The initial orientations of the back shell and the liner were positioned anatomically at a 45°inclination angle while the back shell was fully constrained at its outer surface. The centre of the femoral head was coincided with the centre of the cup, where the centre of a Cartesian coordinates was also located(Fig.1(a)).Only normal walking gait from Kang et al.[20] was considered in the simulation and the corresponding motion and loading conditions were applied at the center of the head including both flexion-extension (FE) abduction-adduction (AA) and internal-external rotation (IER) and three-dimensional forces. Besides, the stem was given three initial angles, defined by FE:25.06°, AA:1.33°, IER:0° so that it corresponded to the beginning position of the walking gait.

The Abaqus/Explicit dynamic method(one method of the commercial finite element software Abaqus version 6.10) was used in the simulation due to its excellent ability to simulate the complex contact problems of artificial hip implants. Because the elasticity modulus of CoCrMo alloy is two orders of magnitude higher than that of UHMWPE, both the head and the back shell were treated as rigid while the liner was considered as an elastic-plastic body. The back shell was meshed with 8-node structured hexahedral element(about 65700 elements) and the element size was about 0.4 mm. The head was meshed by 8-node structured hexahedral element while the stem was discretised using 4-node free tetrahedral element with 0.4 mm and approximate 2.4 mm element size (about 174100 8-node elements, 24800 4-node elements), respectively. The liner was also discretised using 8-node structured hexahedral element,

however different element sizes from 1.25 mm, 1.5 mm and 2 mm were chosen to check the mesh sensitivity and finally 1.5 mm was determined to be appropriate(approximate 6400 elements). Two face-to-face contact pairs were established using the kinematic contact method (outer contact pairs between the back shell inner and the liner outer surfaces, inner contact pairs between the liner inner and head outer surfaces; Abaqus version 6.10). The gait cycle was divided into 41 instants. For each interval, three different time increments (0.01 s, 0.025 s, 0.05 s) were investigated to ensure the convergence, finally 0.025 s was determined. In addition, multiple gait cycles were simulated to investigate the dynamic effect and eventually the first cycle simulation was used as the output results.

The nominal condition for the simulation was defined as a zero clearance at the outer interface and a friction coefficient of 0.08 at both the inner and the outer interfaces. To a dual mobility hip implant, both the inner and outer surfaces of the UHMWPE liner could experience frictional torque. The rotation of the liner would depend on whether its inner surface torque was higher than its outer surface torque. A simple theoretical estimation was made to determine a critical friction coefficient ratio of the inner to the outer interface(the value was 1.43 for the designing geometry of the present dual mobility hip implant). Therefore, the liner would rotate if the friction coefficient ratio was greater than 1.43 and otherwise would be kept static. A fixed friction coefficient of 0.08 was assumed for the inner articulation[21]. The friction coefficient at the outer articulation was assumed to vary from 0.08, 0.065 to 0.05 to investigate its influence, corresponding to friction coefficient ratios of the inner to the outer interfaces of 1, 1.23 and 1.6

respectively.

Clearances at the articulating surfaces could facilitate the relative sliding, whereas interference would prevent their relative movement. However, the clearance or interference between the liner and the metal shell is not generally known. Therefore, different clearances and interferences between the liner and the metal back were considered. A range of radial clearances from 25, 50 and 90 μm was modeled between the liner and the metal back at two kinds of fixed friction coefficient ratios of 1.40 and 1.0(less than the critical value of 1.43), under which condition the liner would be kept static for a zero clearance. Different interferences were also considered, from 25, 50 and 90 μm between the liner and the back shell at a fixed friction coefficient ratio of 1.48 (larger than the critical value).

Before the dynamics simulation of the dual mobility hip implant, the present conceptual model was slightly modified to just consider the inner articulation as a simple ball-in-socket model with different geometric parameters[22] to check the predicted relative sliding distance at the inner articulation(Fig.1(c) and (d)). The radius of the head was 14 mm, and the inner and outer radius of the cup were 14.1 mm and 22.1 mm, respectively.

3. Results

Element sizes and time increments were checked firstly to ensure the solution convergence as detailed in Section 2. The convergent models were then used firstly to checked the predicted sliding distance at the inner articulation and then subsequently the dynamics of the dual mobility hip implant. Fig.

2 shows the comparison of the predicted sliding distance between the present method and that using the method by Kang et al.(2006). Relatively good agreement was obtained, with maximum errors generally being less than 3%. The distributions of the inner and outer contact pressure and accumulated sliding distance under the nominal condition are shown in Fig.3(a)-(d). Under this condition, the liner was kept almost static and the motion mainly occurred at the inner articulation. The inner and outer contact pressure distributions varied over time during the whole gait, the maximum contact pressure being 13.73 MPa and 7.18 MPa, respectively. The inner accumulated sliding distance gradually increased with time and reached the maximum value 19.92 mm at the last instant. However, the outer accumulated sliding only reached 0.72 mm at the first two instants and then nearly kept unchanged in the remaining cycle. Both the inner and outer accumulated sliding distance distributed continuously over the bearing surfaces except a fraction in the center of the outer contact area.

Fig.4(a)-(d) show the distributions of the inner and outer contact pressure and accumulated sliding distance when the friction coefficient ratio of the inner to the outer interface was 1.6. Under this condition, the rotation of the liner occurred. The variations of the inner and outer contact pressure distribution were similar to those obtained from the nominal condition, and the inner and outer maximum contact pressure values were 13.54 MPa and 7.50 MPa. The relative sliding between the liner and the head was small under this condition, with a maximum value of 1.22 mm. However, the outer accumulated sliding distance increased over time and reached the maximum value of 29.20 mm in one cycle. Moreover, both

the inner and outer accumulated sliding distance distributions were continuous.

The results of the inner and outer maximum contact pressure under different friction coefficient ratios are shown in Fig.5(a) and (b), respectively. Both the inner and outer maximum contact pressure varied with the applied load in each instant and reached their maximum values at 65% gait where the corresponding maximum load of 2200 N was applied. Different friction coefficient ratios resulted in negligible differences in the predicted maximum contact pressure at both the inner and outer interfaces. The inner and outer maximum accumulated sliding distances under different friction coefficient ratios are shown in Fig.6(a) and (b), respectively. When the friction coefficient ratios of the inner to the outer interface were 1 and 1.23, the liner was kept static and its inner and outer maximum accumulated sliding distances at each instant were nearly the same, about 19.9mm and0.9mm over the entire gait cycle. However, with the friction coefficient ratio of 1.6, the liner rotated with the head and its outer maximum accumulated sliding distance increased rapidly over time and reached the maximum value of 29.20 mm while the inner maximum sliding distance remained unchanged with a maximum value of 1.22 mm.

Fig.7(a) and (b) show the contact area at the inner and outer interfaces under different friction coefficient ratios. There were no large differences in the inner contact area under this condition. For the outer interface, the contact area was slightly lower when dual rotation occurred than that of only inner rotation. The maximum inner contact area was about 320 mm^2 while the maximum outer contact area achieved 820 mm^2.

For different initial clearances between the liner and the back shell, the maximum accumulated sliding distance of the inner and outer interfaces are shown in Fig.8 for a friction coefficient ratio of 1.40. Under the nominal conditions, the primary motion would occur at the inner articulation. Increasing the clearance resulted in an increased tendency for the outer articulation to occur. It is clear that the maximum accumulated sliding distance of the inner articulation decreased markedly when the initial clearance increased, and the maximum value decreased from 19.69 mm to 12.68 mm in the last instant. On the other hand, the maximum accumulated sliding distance of the outer interface increased at the same instant while the initial clearance was increased, and the maximum value increased from 1.26 mm to 12.22 mm. Fig.9 shows the results of the liner inner and outer contact area for different initial clearances between the liner and the back shell. The liner inner contact area did not vary largely for different initial clearances. However the liner outer contact area decreased noticeably at the same instant when the initial clearance was increased. The maximum contact area of the outer interface decreased from 815 mm^2 to 423 mm^2 over the entire gait cycle. Different clearances resulted in negligible differences in the predicted contact area at the inner articulation, while an approximately twofold difference at the outer articulation was found. Different clearances were also considered under a fixed friction coefficient ratio of 1.0, the comparisons of maximum contact pressure of liner inner and outer surface between this ratio and the ratio of 1.40 are listed in Table 2. Under the friction coefficient ratio of 1.0, neither the maximum contact pressure or the accumulated sliding distance showed marked difference for all clearance setup, and the

mean maximum accumulated sliding distance of the inner liner was much higher than that of the outer liner (about 19.90 mm vs 0.65mm, and the result of maximum accumulated sliding distance distribution was not shown).

Comparisons of both the liner inner and outer maximum accumulated sliding distance for different initial interferences between the liner and the back shell are made in Fig.10 for a friction coefficient ratio of 1.48. The liner rotated with the head when there was no initial interference between the liner and the back shell, and nearly no relative sliding between the liner and the head. The maximum accumulated sliding distance of the inner articulation was only 4.42 mm while the corresponding value of the outer reached 24.54 mm. Introducing the interference led to the liner static; the maximum inner accumulated sliding distance gradually increased to about 19.71 mm, however the corresponding value of the outer was only about 1.40 mm. Different initial interferences from 25 to 90 μm resulted in negligible differences in the predicted inner and outer maximum accumulated sliding distances. As to the liner inner and outer maximum contact pressure, there were little differences for different initial interferences between the liner and the back shell, and the inner and outer articulation maximum contact pressure were about 13.68 MPa and 9.78 MPa, respectively (results not shown). In addition, different initial interferences between the liner and the back shell did not result in marked differences of both the inner and outer articulating surface contact area, and the corresponding maximum contact area were about 328 mm^2 and 998 mm^2 (results not shown) .

4. Discussion

The dynamic contact simulation of a conceptual dual mobility hip implant was successfully developed in the present study. The direct experimental validation of the present model was beyond the scope of the present study. A number of attempts were made to ensure the validity of the model; including the mesh sensitivity study and the comparison of the predicted relative sliding distance with a previous study[22]. Such a dynamics contact model is able to predict contact pressure and contact area as well as accumulated sliding distance. Although this method has been widely used for artificial knee joints[23, 24],the present study is the first application of dynamic contact mechanics simulation to dual mobility hip implants. This differs from most previous finite element studies of conventional artificial hip joints using Abaqus/Standard approach which only allows the static contact mechanics examined[25, 26]. For dual mobility hip implants, it is necessary to apply such a dynamic contact mechanics model.

The dual mobility hip implants could experience two different typical motions for different friction coefficient ratios of the inner to the outer articulations and different initial clearances/interferences between the liner and the back shell. The rotation of the liner with the head mainly depended on whether the frictional torque at the inner articulation exceeded the corresponding value at the outer articulation. The liner rotated with the head when the inner torque was higher than its outer torque, otherwise the liner would be kept static. There existed a critical friction coefficient ratio to determine the dual motion of the dual mobility hip implant. For the geometry of the dual mobility hip implant considered, a theoretical

value of the critical friction coefficient ratio between the inner and the outer articulations was calculated as 1.43. This value was quite close to the critical friction coefficient ratio of 1.45 simulated by the present finite element analysis. Such a small difference was mainly a result of neglecting the clearance between the liner and the head in the theoretical analysis, which would facilitate the rotation at the outer articulation. The effects of different friction coefficient ratios on the motions of the liner were broadly in agreement with those of Rowe et al.[27]. These authors found that only the head rotated if a lubricant was used at the inner contact pair or at both inner and outer contact pairs, but the liner rotated with the head if a lubricant was used just at outer contact pair. In addition, design parameters could also influence how the liner rotated. Increasing the initial clearance between the liner and the back shell would gradually facilitate the liner rotate with the head when the friction coefficient of ratio was a bit lower than the predicted critical value(1.45); when the friction coefficient of ratio was close to 1.0, the inner motion predominated in dual mobility hip implant even the clearance reached 90 micro meters. From long-term, both the poly polyethylene ages and in-time wear would increase clearance of both inner and outer articulate interface. When clearance becomes much larger than initial value, the dual mobility rotation may be easier to occur for dual mobility hip implant. Besides, if interference exists at outer articulate interface, even a small initial interference of 25 μm could prevent the rotation of the liner.

The liner motion status would directly determine the magnitude of accumulated sliding distance of both two pairs of articulating surfaces. Under the condition when the liner was kept static, the inner

sliding distance increased over the gait cycle while the outer sliding distance was small. On the contrary when the liner rotated, the outer sliding distance increased while the inner sliding distance was minimum. Furthermore, the outer maximum accumulated sliding distance when the liner rotated with the head was much higher than the inner maximum accumulated sliding distance when the liner was kept static, the ratio between them was roughly 1.5.

Both different friction coefficient ratios and different initial clearances/interfaces did not result in marked differences in the inner and outer interfaces contact pressure, but indeed induced the different motions and eventually led to the change of contact zone. In addition, under these different conditions, the inner interface contact pressure were much higher than the outer interface contact pressure(about 2 times). As to contact area, the change of friction coefficient ratio and initial interference between the liner and the back shell did not result in obvious differences both in the inner and outer interface contact area. However, the increasing of initial clearance between the liner and the back shell largely decreased the outer interface contact area without apparently influencing the inner interface contact area. Nevertheless, under both different friction coefficient ratio and different initial clearances/interferences, the outer interface contact area was much higher than the inner interface contact area.

Wear of UHMWPE cups depends on sliding distance and pressure[28] and the contact area[29]. Therefore, it would probably result in extensive wear if the liner rotates with the head due to a larger sliding distance and contact area even though the contact pressure is low, compared with when only the head rotates. For a

typical dual mobility hip implant, current material combinations would not lead to the inner articulation torque exceeding the outer articulation[21], and no initial clearances/interferences have been reported at the outer articulation. Under these conditions, only the head would rotate during normal walking gait and mainly the inner articulation wear would occur, which is consistent with the wear tests obtained by Saikko[11] and Loving[30]. However, under abnormal conditions such as a high friction coefficient ratio between the inner and the outer interfaces or initial clearance (either as a result of design or wear) in the outer articulating interface, the liner would rotate with the head even during normal walking gait. This may eventually lead to extensive wear of the outer articulating surface because of large sliding distance coupled with large contact area.

Although the motion of a typical dual mobility hip implant under normal walking gait was studied in this study, the effect of other activities and gait patterns remains unclear. Therefore, it is necessary to investigate the dynamics and contact mechanics of dual mobility hip implants in future under other daily movements such as upstairs, downstairs as well as standing up. Besides, the actual friction coefficient of ratio is needed to be further investigated to determine the effect of clearance on the motion of dual mobility hip implant. Moreover, the clinical results of the primary motion pattern correspondence to various clearance designs should also be investigated. In clinical, the long-term reasons including in-time wear and polyethylene ages which would affect clearance of dual mobility hip implant also need to be investigated in future. The capsule or pseudo-capsule could affect motion of dual mobility hip implant,

this will be study in future. In addition, the possible influence of inclination of the liner on motion of dual mobility hip implant should also be considered in future to provide useful advices to surgeons. wear Experimental studies should also been carried out in the future research to validate the present finite element modeling as well as integrating dynamics, contact mechanic and wear of dual mobility hip implants.

5.Conclusions

The kinematics and contact mechanics of a typical dual mobility hip under different friction coefficient ratios between the inner and outer articulations and initial clearances/interferences between the liner and the back shell were simulated using Abaqus/Explicit dynamic module. The motion of the dual mobility hip was highly dependent on friction coefficient ratios and initial clearances/interferences between the liner and the back shell. The liner remained static if the friction coefficient ratio was lower than the critical ratio of 1.45 for the geometry considered, otherwise it rotated with the head. An initial clearance of 25 μm between the liner and the back shell would contribute to the rotation of the liner if the ratio of friction coefficient was close to the predicted critical value(1.45). Similarly, even a small initial interference of 25 μm between the liner and the back shell could prevent the rotation of the liner. The outer articulating sliding distance when the liner rotated with the head was much higher, compared with the inner articulation sliding distance if the liner was kept static. The motions of the dual mobility hip implant would not apparently influence the inner and outer articulating contact pressure. The inner

articulation average contact pressure was about three times higher than the outer articulation average contact pressure, whereas the outer articulation contact area was much higher than the inner articulation contact area.

Acknowledgements

The work has been supported by both the State Key Laboratory for Manufacturing System Engineering and National Science and Technology Major Project of China and "the Fundamental Research Funds for Central Universities". the Program of the National Nature Science foundation of China [grants number 51205303], National Science and Technology Supporting Program [grants number 2012BAI18B00], National Science Foundation Project of China [grants number 81301564; 51323007].

References

1. Dressler M.R, Strickland M.A, Taylor M, Render T.D, Ernsberger CN. Predicting wear of UHMWPE: Decreasing wear rate following a change in direction. *Wear*. 2011; 271: 2879-83.

2. Mattei L, Di Puccio F, Piccigallo B, Ciulli E. Lubrication and wear modelling of artificial hip joints: A review. *Tribology International*. 2011; 44: 532-49.

3. Banchet V, Fridrici V, Abry J.C, Kapsa P. Wear and friction characterization of materials for hip prosthesis. *Wear*. 2007; 263: 1066-71.

4. Prokopetz J.J, Losina E, Bliss R.L, Wright J, Baron J.A, Katz J.N. Risk factors for revision of primary total hip arthroplasty: a systematic review. *BMC Musculoskelet Disord* 2012; 13: 251 (accessed 2012).

5. Adam P, Philippe R, Ehlinger M, et al. Dual mobility cups hip arthroplasty as a treatment for displaced fracture of the femoral neck in the elderly. A prospective, systematic, multicenter study with specific focus on postoperative

dislocation. *Orthop Traumatol Surg Res*. 2012; 98: 296-300.

6. Guyen O, Chen Q.S, Bejui-Hugues J, Berry D.J, An K.N. Unconstrained tripolar hip implants: effect on hip stability. *Clin Orthop Relat Res*. 2007; 455: 202-8.

7. Philippeau J.M, Durand J.M, Carret J.P, Leclercq S, Waast D, Gouin F. Dual mobility design socket use in preventing total hip replacement dislocation following tumor resection. *Orthopaedics & Traumatology: Surgery & Research*. 2010; 96: 2-8.

8. Stroh A, Naziri Q, Johnson A.J, Mont M.A. Dual-mobility bearings: a review of the literature. *Expert review of medical devices*. 2012; 9: 23-31.

9. Geringer J, Boyer B, Farizon F. Understanding the dual mobility concept for total hip arthroplasty. Investigations on a multiscale analysis-highlighting the role of arthrofibrosis. *Wear*. 2011; 271: 2379-85.

10. Adam P, Farizon F, Fessy M.H. Dual articulation retentive acetabular liners and wear: surface analysis of 40 retrieved polyethylene implants. *Rev Chir Orthop Reparatrice Appar Mot*. 2005; 91: 627-36.

11. Saikko V, Shen M. Wear comparison between a dual mobility total hip prosthesis and a typical modular design using a hip joint simulator. *Wear*. 2010; 268: 617-21.

12. Loving L, Lee R.K, Herrera L, Essner A.P, Nevelos J.E. Wear performance evaluation of a contemporary dual mobility hip bearing using multiple hip simulator testing conditions. *J Arthroplasty*. 2013; 28: 1041-6.

13. Rowe S.M, R. Y.T, P. H.J. Clinical experience of a new bipolar hip prosthesis. *Chonnam J Med Sci*. 1994; 7: 9.

14. Rowe S.M, Chung J.Y, Moon E.S, Yoon T.R, Seo H.Y, Lee J.J. Why does outer joint motion predominate in bipolar hip prosthesis? Experimental and clinical studies. *Acta Orthop Scand*. 2004; 75: 701-7.

15. Fabry C, Kaehler M, Herrmann S, Woernle C, Bader R. Dynamic behavior of tripolar hip endoprostheses under physiological conditions and their effect on stability. *Medical engineering & physics*. 2013.

16. Geringer J, Boyer B, Farizon F. Understanding the dual mobility concept for total hip arthroplasty. Investigations on a multiscale analysis-highlighting the role of arthrofibrosis. *Wear*. 2011; 271: 2379-85.

17. Jin ZM, Heng S.M, Ng H.W, Auger D.D. An axisymmetric contact model of ultra high molecular weight

polyethylene cups against metallic femoral heads for artificial hip joint replacements. *Proceedings of the Institution of Mechanical Engineers Part H, Journal of engineering in medicine*. 1999; 213: 317-27.

18. Fregly B.J, Bei Y, Sylvester M.E. Experimental evaluation of an elastic foundation model to predict contact pressures in knee replacements. *Journal of biomechanics*. 2003; 36: 1659-68.

19. Kluess D, Martin H, Mittelmeier W, Schmitz K.P, Bader R. Influence of femoral head size on impingement, dislocation and stress distribution in total hip replacement. *Medical engineering & physics*. 2007; 29: 465-71.

20. Kang L, Galvin A.L, Jin ZM, Fisher J. A simple fully integrated contact-coupled wear prediction for ultra-high molecular weight polyethylene hip implants. *Proc Inst Mech Eng H*. 2006; 220: 33-46.

21. Banchet V, Fridrici V, Abry J.C, Kapsa P. Wear and friction characterization of materials for hip prosthesis. *Wear*. 2007; 263: 1066-71.

22. Kang L, Galvin A.L, Jin ZM, Fisher J. A simple fully integrated contact-coupled wear prediction for ultra-high molecular weight polyethylene hip implants. *Proceedings of the Institution of Mechanical Engineers Part H, Journal of engineering in medicine*. 2006; 220: 33-46.

23. Godest A.C, Beaugonin M, Haug E, Taylor M, Gregson P.J. Simulation of a knee joint replacement during a gait cycle using explicit finite element analysis. *Journal of biomechanics*. 2002; 35: 267-75.

24. Halloran J.P, Petrella A.J, Rullkoetter P.J. Explicit finite element modeling of total knee replacement mechanics. *J Biomech*. 2005; 38: 323-31.

25. Udofia I.J, Yew A, Jin ZM. Contact mechanics analysis of metal-on-metal hip resurfacing prostheses. *Proc Inst Mech Eng H*. 2004; 218: 293-305.

26. Liu F, Leslie I, Williams S, Fisher J, Jin Z. Development of computational wear simulation of metal-on-metal hip resurfacing replacements. *J Biomech*. 2008; 41: 686-94.

27. Rowe S.M, Chung J.Y, Moon E.S, Yoon T.R, Seo H.Y, Lee J.J. Why does outer joint motion predominate in bipolar hip prosthesis? Experimental and clinical studies. *Acta orthopaedica*. 2004; 75: 701-7.

28. Maxian T.A, Brown T.D, Pedersen D.R, Callaghan J.J. A sliding-distance-coupled finite element formulation

for polyethylene wear in total hip arthroplasty. *Journal of biomechanics*. 1996; 29: 687-92.

29. Liu F, Galvin A, Jin Z, Fisher J. A new formulation for the prediction of polyethylene wear in artificial hip joints. *Proc Inst Mech Eng H*. 2011; 225: 16-24.

30. Loving L, Lee R.K, Herrera L, Essner A.P, Nevelos J.E. Wear performance evaluation of a contemporary dual mobility hip bearing using multiple hip simulator testing conditions. *The Journal of arthroplasty*. 2013; 28: 1041-6.

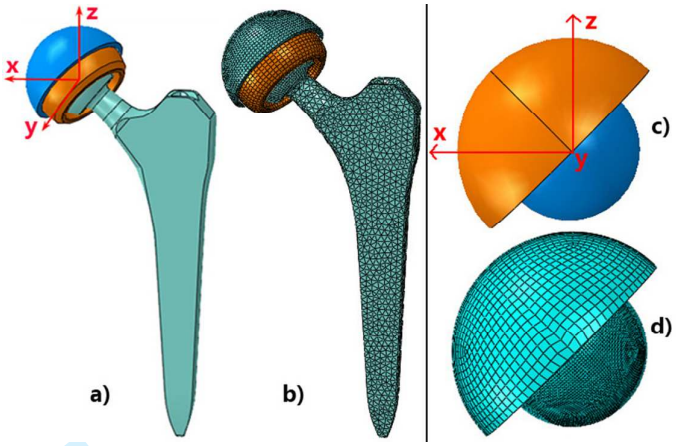

Fig.1 Dual mobility hip model and simple ball-in-socket model (a) CAD model of dual mobility hip model (b) FE model of dual mobility hip model (c) CAD model of ball-in-socket model (d) FE model of ball-in-socket model

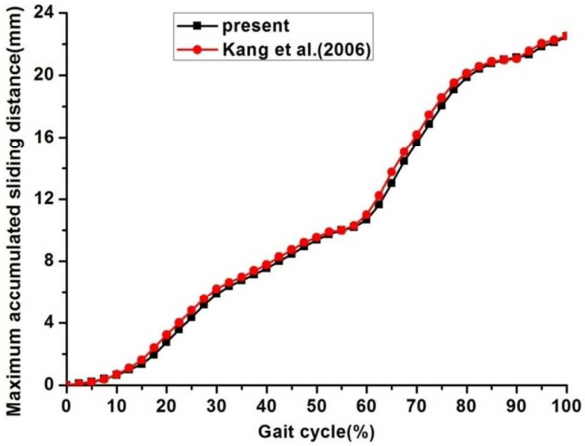

Fig.2 Comparison of maximum sliding distance of the simple ball-in-socket model with that using the method by Kang(2006)

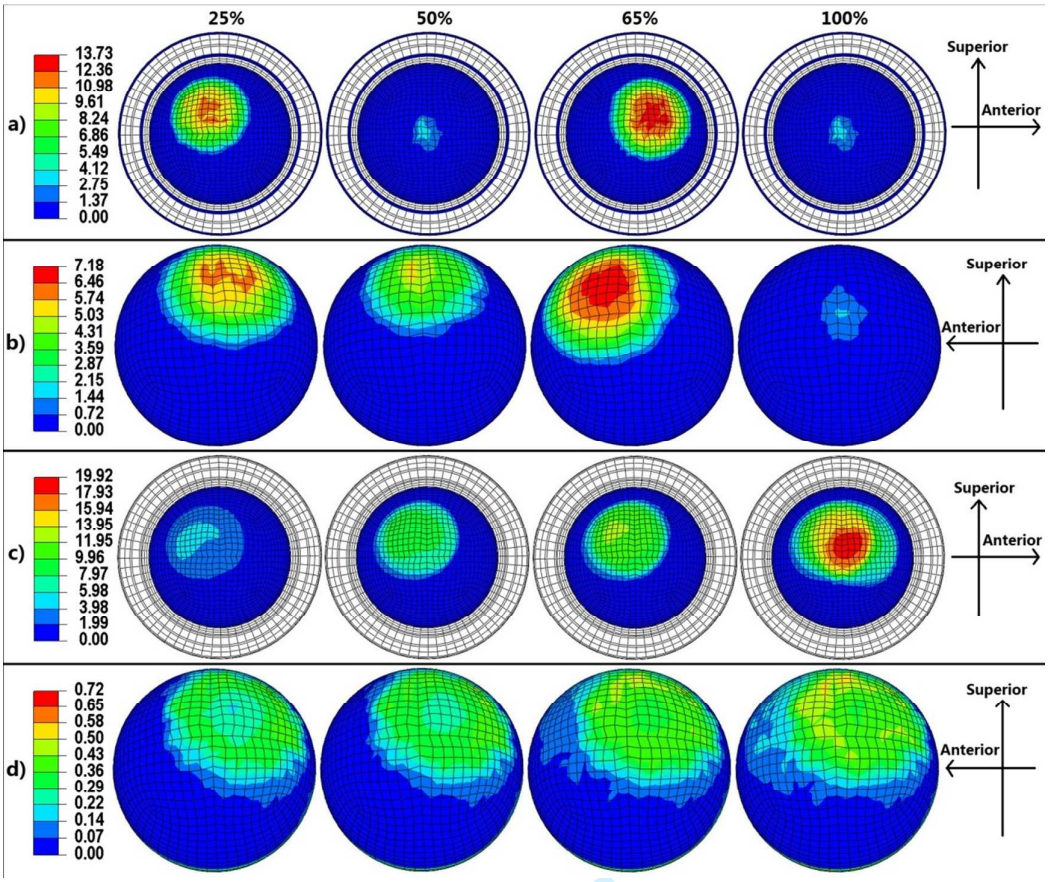

Fig.3 Contours of the liner contact pressure and accumulated sliding distance under a friction coefficient ratio of 1 during different walking instants (a) Inner contact pressure(MPa) (b) Outer contact pressure(MPa) (c) Inner accumulated sliding distance(mm) (d) Outer accumulated sliding distance(mm)

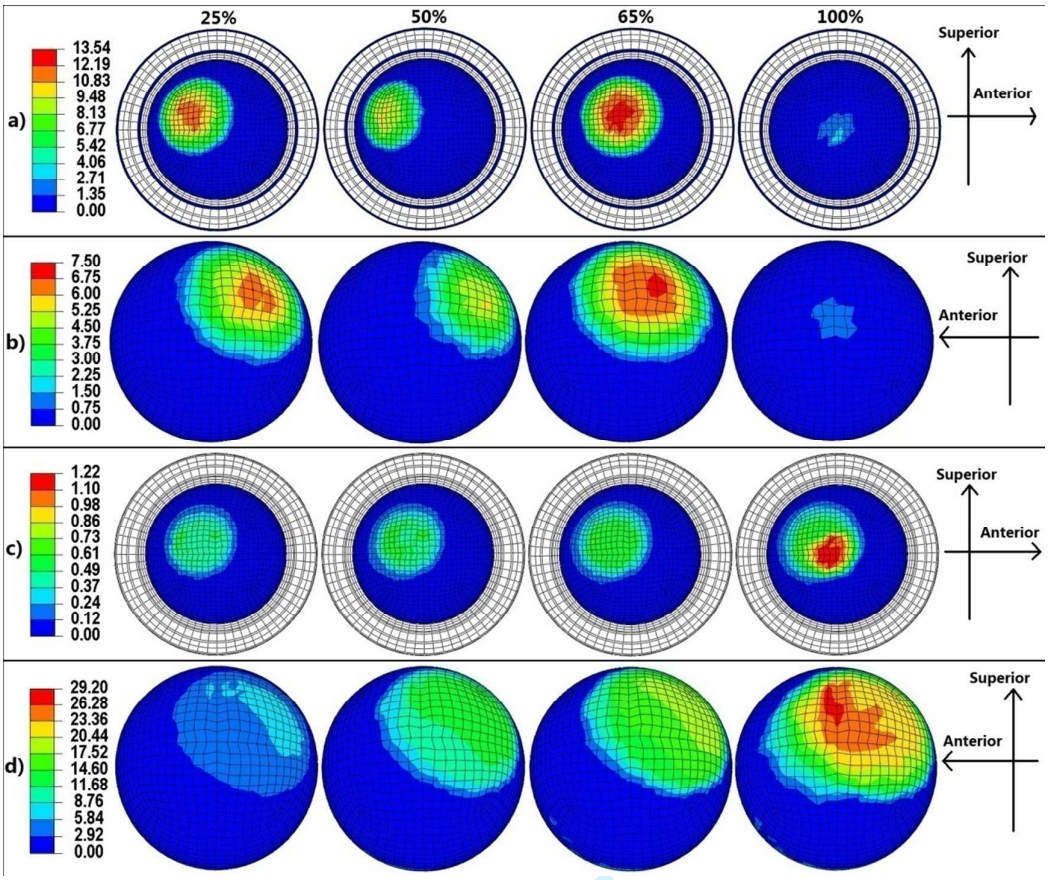

Fig.4 Contours of the liner contact pressure and accumulated sliding distance under a friction coefficient ratio of 1.6 during different walking instants (a) Inner contact pressure(MPa) (b) Outer contact pressure(MPa) (c) Inner accumulated sliding distance(mm) (d) Outer accumulated sliding distance(mm)

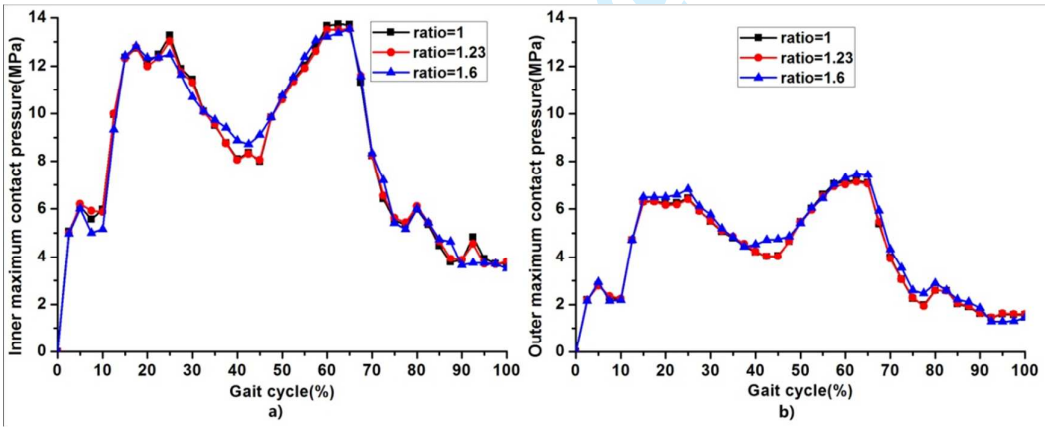

Fig.5 Maximum contact pressure of the liner as a function of the gait cycle under different friction coefficient ratios of the inner to the outer articulation (a) Inner maximum contact pressure (b) Outer maximum contact pressure

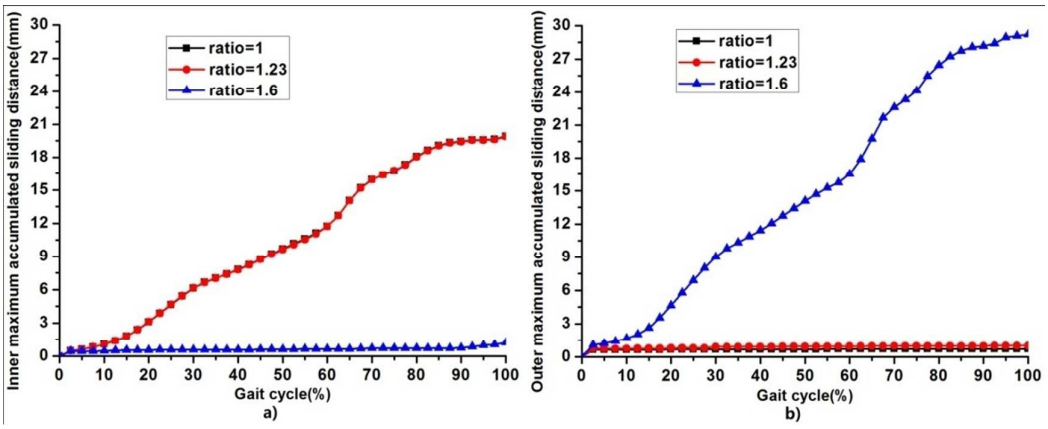

Fig.6 Maximum accumulated sliding distance of the liner as a function of the gait cycle under different friction coefficient ratios of the inner to the outer articulation (a) Inner maximum accumulated sliding distance (b) Outer maximum accumulated sliding distance

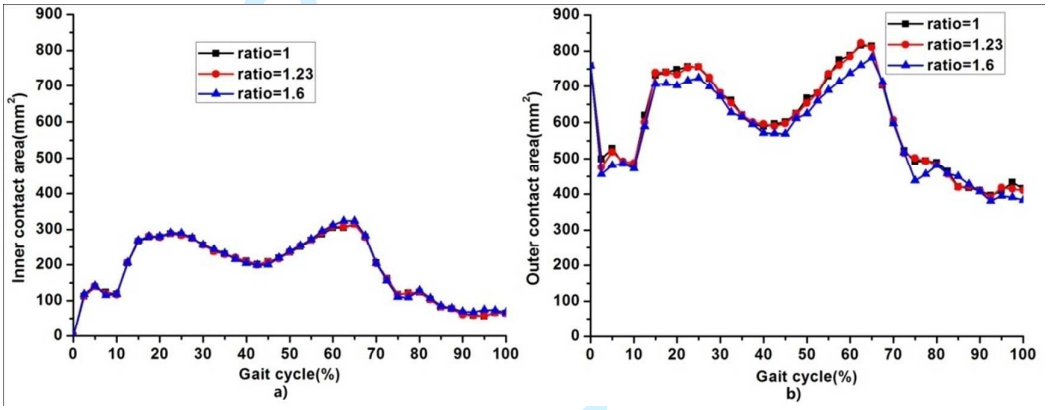

Fig.7 Contact area of the liner as a function of the gait cycle under different friction coefficient ratios of the inner to the outer articulation (a) Inner contact area (b) Outer contact area

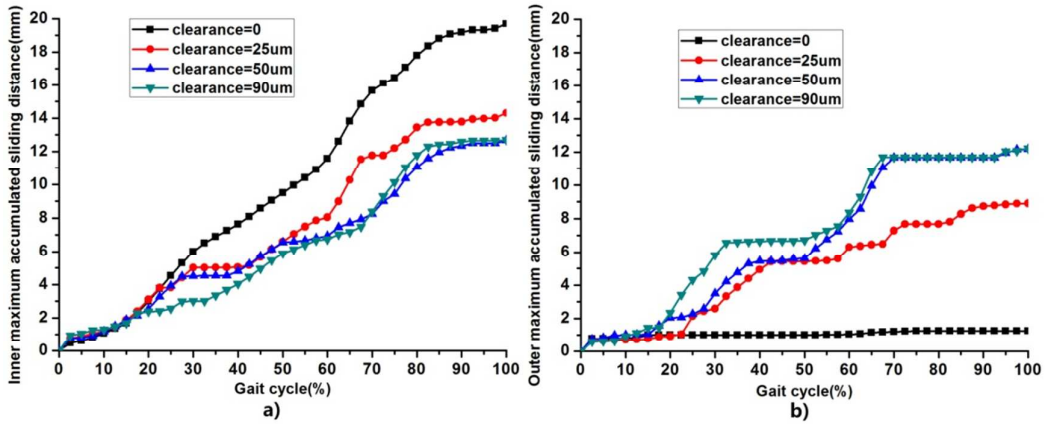

Fig.8 Maximum accumulated sliding distance of the liner as a function of the gait cycle under different initial clearances of the outer articulation and a fixed friction coefficient ratio of 1.40 (a) Inner maximum accumulated sliding distance (b) Outer maximum accumulated sliding distance

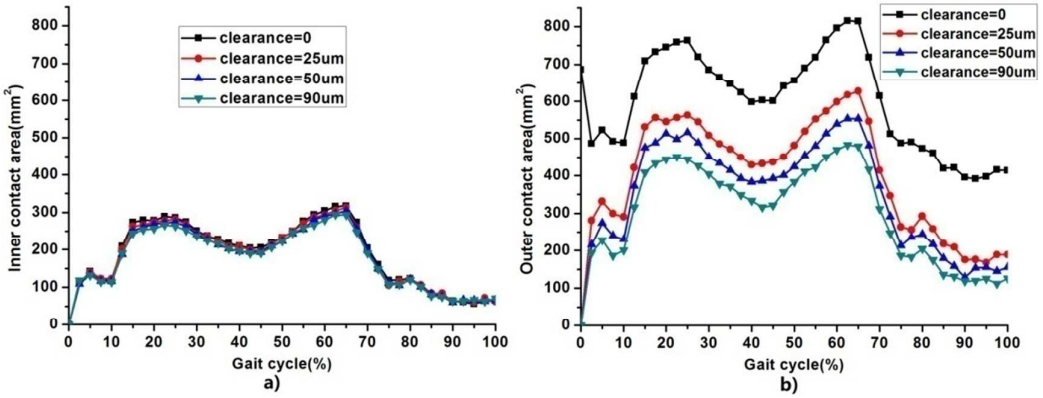

Fig.9 Contact area of the liner as a function of the gait cycle under different initial clearances of the outer articulation and a fixed friction coefficient ratio of 1.40 (a) Inner contact area (b) Outer contact area

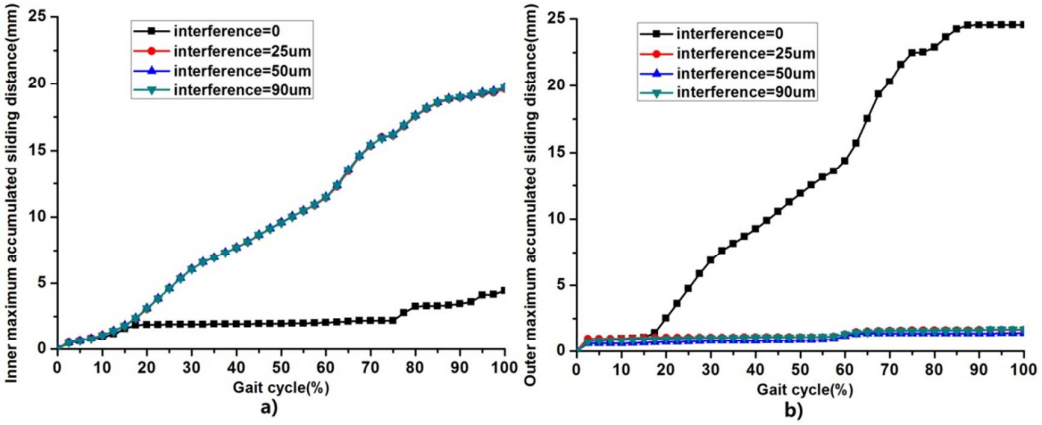

Fig.10 Maximum accumulated sliding distance of the liner as a function of the gait cycle under different initial interferences of the outer articulation and a fixed friction coefficient ratio of 1.48 (a) Inner maximum accumulated sliding distance (b) Outer maximum accumulated sliding distance

Table 1 CAD model and FE model key parameters of dual mobility hip

	Inner radius(mm)	Outer radius(mm)	Materials	Density (g/mm^{3})	Elastic modulus (GPa)	Poisson's ratio
Head	\	14.0	CoCrMo	7.61	217	0.30
Liner	14.1	20.0	UHMWPE	9.32e-1	1	0.45
Back	20.0	23.0	CoCrMo	7.61	217	0.30

Table 2 Contour plot of the maximum contact pressure(MPa) distribution of the liner inner and outer surfaces under combined clearance and ratio of two articulations for dual mobility hip

		Clearance(um)			
		0	25	50	90
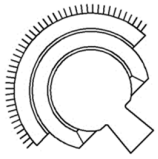 Ratio=u_{inner}/u_{outer} Liner inner	1.4	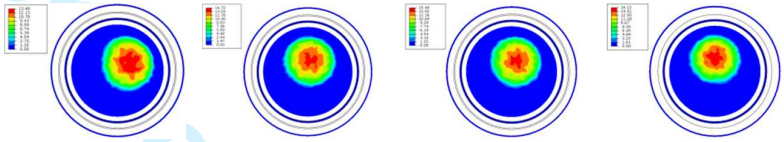 13.48	14.72	15.48	16.12
	1.0	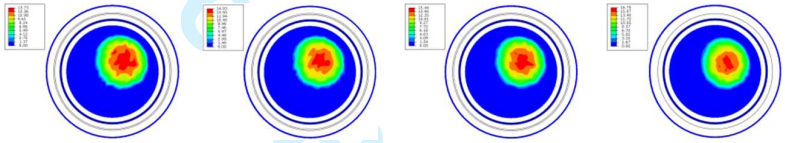 13.73	14.93	15.44	16.75
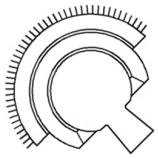 Ratio=u_{inner}/u_{outer} Liner outer	1.4	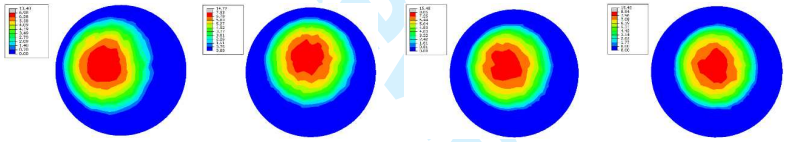 6.90	7.53	8.05	8.84
	1.0	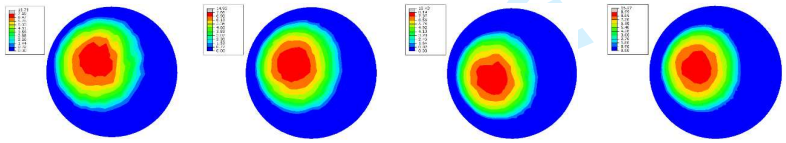 7.19	7.66	8.19	8.99